Perturbations of ionization fractions at the cosmological recombination epoch

B. Novosyadlyj*

Astronomical Observatory of the Ivan Franko National University of Lviv, Kyryla i Methodia str., 8, Lviv, 79005, Ukraine

Accepted 2006 May 17 . Received 2006 March 22

ABSTRACT

A development of perturbations of number densities of ions and electrons during recombination epoch is analysed. The equations for relative perturbations of ionization fractions were derived from the system of equations for accurate computation of the ionization history of the early Universe given by Seager et al. (1999, 2000). It is shown that strong dependence of ionization and recombination rates on the density and temperature of plasma provides the significant deviations of amplitudes of ionization fractions relative perturbations from ones of baryon matter density adiabatic perturbations. Such deviations are most prominent for cosmological adiabatic perturbations of scales larger than sound horizon at recombination epoch. The amplitudes of relative perturbations of number densities of electrons and protons at last scattering surface exceed by factor of $\simeq 5$ the amplitude of relative perturbation of baryons total number density, for helium ions this ratio reaches the value of $\simeq 18$. For subhorizon cosmological perturbations these ratios appear to be essentially lesser and depend on oscillation phase at the moment of decoupling. These perturbations of number densities of ions and electrons at recombination epoch do not contribute to the intrinsic plasma temperature fluctuations but cause the "corrugation" of last scattering surface in optical depth, $\delta z_{dec}/(z_{dec}+1) \approx -\delta_b/3$, at scales larger than sound horizon. It may result into noticeable changes of precalculated values of CMB polarization pattern at several degrees angular scales.

Key words: cosmology: theory—early Universe—atomic processes—cosmic microwave background

INTRODUCTION

Cosmic microwave background (CMB) radiation coming from recombination epoch has become one of the most powerful observational probes for cosmological models of our Universe and formation of its large-scale structure. Indeed, the full-sky maps of cosmic microwave temperature fluctuations obtained by Wilkinson Microwave Anisotropy Probe (WMAP) during first year of observations have given a possibility to determine the cosmological parameters with high accuracy, $\sim 2\%$ (Bennet et al. 2003; Verde et al. 2003; Spergel et al. 2003). The current data from three year of WMAP observations (Spergel et al. 2006) and, especially, expected from future mission Planck, improve precision of the CMB power spectrum determination to the level of accuracy of numerical precalculations done by the most advanced codes in the framework of specific model. For example, CMBfast code by Seljak & Zaldarriaga (1996); Zaldarriaga & Seljak (1999) has intrinsic accuracy $\simeq 1\%$. An adequate calculation of the recombination process is crucial for modelling the power spectrum of CMB temperature fluctuations and polarization.

The first analyses of recombination kinetics were carried out by Zel'dovich, Kurt & Sunyaev (1968) and Peebles (1968) in 1967. In subsequent papers (Matsuda, Sato & Takeda 1971; Zabotin & Nasel'skii 1982; Liubarskii & Sunyaev 1983; Hummer & Storey 1998; Krolik 1990; Rubicki & Dell'Antonio 1993 and citing therein) the main processes have been studied using the 3-level approximation of hydrogen and helium atoms. An accuracy of few percents has been achieved. The most complete analysis of cosmological recombination processes with taking into account the multi-level structure of hydrogen and helium atoms ($\simeq 300$ levels) and non-equilibrium ionization-recombination kinetics has been performed by Seager, Sasselov

& Scott (2000). Also all known plasma thermal processes were taken into account therein. These authors have provided cosmological community with software RECFAST (Seager et al. 1999) which ensures an accuracy of calculation of number density of electrons $\sim 1\%$. This code was used by number of authors to calculate the transfer function of density perturbations and power spectrum of CMB temperature fluctuations and polarization, in particular, by Seljak & Zaldarriaga (1996); Zaldarriaga & Seljak (1999) for publicly available software CMBFAST. However, the researches aimed on improving the calculation of recombination and decoupling of the thermal radiation from baryon plasma are still going on (see recent papers by Dubrovich & Grachev (2005); Chluba & Sunyaev (2006); Kholupenko, Ivanchik & Varshalovich (2005); Wong, Seager & Scott (2005) and citing therein).

In this paper the evolution of number density perturbations of hydrogen and helium ions and electrons in the field of cosmological matter density perturbations is studied. The cosmological adiabatic perturbations closely associate the density and temperature variations in baryon-radiation component, leading to the corresponding variations of photorecombination and photoionization rates, which in turn can cause appreciable deviations of relative perturbation amplitudes of number density of ions and electrons from corresponding amplitude for total number density of baryon nuclei. The effective 3-level models of hydrogen and helium atoms by Seager et al. (1999) and their software RECFAST were used as a basis. Here all calculations were carried out for z > 100 when recombination and dissociation processes of hydrogen negative ions H^- and molecules H_2 and H_2^+ can be neglected due to their insignificance.

In the first section the basic equations for hydrogen and helium recombination in homogeneous expanding Universe are presented along with their numerical solutions for Λ CDM model. The definitions of relative perturbations of number densities of ions and electrons, their properties, equations for their evolution and results of integration for the stationary mass density and temperature initial perturbations are given in the second section. The third section is devoted to the analysis of perturbations of electron number density within the adiabatic mass density perturbations of different scales in Λ CDM model. An estimation of contribution of this effect into the "corrugation" of last scattering surface and CMB temperature fluctuations is carried out in the 4th section.

1 COSMOLOGICAL RECOMBINATION OF HYDROGEN AND HELIUM ATOMS: DEFINITIONS, EQUATIONS, RESULTS

Let us introduce the following definitions: $n_{\rm HI}$ and $n_{\rm HII}$ denote the number densities of neutral and ionized hydrogen atoms respectively, $n_{\rm HeII}$, $n_{\rm HeII}$ and $n_{\rm HeIII}$ – number densities of neutral, singly and double ionized helium atoms, $n_{\rm e} = n_{\rm HII} + n_{\rm HeII} + 2n_{\rm HeIII}$ – number density of free electrons, $n_{\rm H} = n_{\rm HI} + n_{\rm HII}$ – total number density of hydrogen nuclei, $n_{\rm He} = n_{\rm HeI} + n_{\rm HeIII} + n_{\rm HeIII}$ – total number densities (ionizations): $x_{\rm HI} \equiv n_{\rm HII}/n_{\rm H}$ – relative abundance of neutral hydrogen, $x_{\rm HII} \equiv n_{\rm HII}/n_{\rm H}$ – the same for ionized hydrogen, $x_{\rm HeI} \equiv n_{\rm HeI}/n_{\rm He}$, $x_{\rm HeIII} \equiv n_{\rm HeIII}/n_{\rm He}$ – relative abundances of neutral helium, singly and double ionized helium atoms, $x_{\rm e} \equiv n_{\rm e}/n_{\rm H}$ – relative number density of electrons. The ratio of total number densities of helium and hydrogen nuclei we define as $f_{\rm He} \equiv n_{\rm He}/n_{\rm H}$, which can be expressed via mass fraction of primordial helium Y_P , so that $f_{\rm He} = Y_P/4(1-Y_P)$ (further we assume $Y_P = 0.24$ from Schramm & Turner (1998)). This quantities obey evident relationships: $x_{\rm e} = x_{\rm HII} + f_{\rm He}x_{\rm HeII} + 2f_{\rm He}x_{\rm HeIII}$, $x_{\rm HI} + x_{\rm HeII} + x_{\rm HeII} + x_{\rm HeII} = 1$. All following formulae and relations are presented for these relative number densities of atoms, ions and electrons.

As it follows from above cited papers and, in particular, from refined numerical calculations by Seager et al. (1999, 2000) at early stages of universe evolution $(z > 10^4)$ all hydrogen and helium atoms were ionized completely by thermal photons, so, then $x_{\rm HII} = 1$, $x_{\rm HI} = 0$, $x_{\rm HeIII} = 1$, $x_{\rm HeI} = x_{\rm HeII} = 0$ and $x_{\rm e} = 1 + 2f_{\rm He}$. This is a consequence of high number density of thermal high-energy photons capable to rend electrons from all atoms and ions. In the expanding Universe the energy of each photon and temperature of radiation decrease $\propto a^{-1}$, radiation energy density $\propto a^{-4}$, the number and mass density of baryons and dark matter $\propto a^{-3}$, where a is the scale factor which is associated with redshift z by simple relation $a=(z+1)^{-1}$. Already at $z\sim 8000$ thermal photons with energies higher than potentials of ionization of HeII from ground and second levels reside in the short-wave tail of Planck function and their number density becomes too low to keep all helium in the ionization stage of HeIII. It begins to recombine and at $z \sim 7000$ the HeII ions appear. At this moment the time-scale of Thomson scattering $(t_{\rm T} \simeq 3m_e c(1+x_{\rm e}+f_{\rm He})/(8\sigma_{\rm T} a_{\rm R} T_{\rm R}^4 x_{\rm e})$, the hydrogen recombination time-scale $(t_{\rm HI} \simeq 1/n_{\rm e} \alpha_{\rm HI})$ and the helium one $(t_{\text{HeII}} \simeq 1/n_{\text{e}}\alpha_{\text{HeII}})$ appear to be essentially lower in comparison with the time-scale of Universe expansion $(t_{\text{Hubble}} \simeq 2/3H_0(1+z)^{3/2})$. Thus, matter temperature (electronic and ionic one) T_{m} equals to CMB temperature, T_{R} . Recombination of HeII occurs in the conditions of local thermodynamic equilibrium (LTE). In the expressions for time-scales m_e denotes the mass of electron, c is the light speed, $\sigma_{\rm T}$ is the effective cross-section of Thomson scattering, $a_{\rm R}$ is the radiation constant, α_i is the effective coefficients of recombination to the ground states of hydrogen atoms HI and singly ionized helium atoms, HeII. An ionization fraction of helium, x_{HeIII}, is described by Saha equation:

$$\frac{x_{\rm e}x_{\rm HeIII}}{x_{\rm HeII}} = \frac{(2\pi m_{\rm e}kT_m)^{3/2}}{h^3n_{\rm H}} e^{-\chi_{\rm HeII}/kT_m}.$$
(1)

Whereas at this epoch both hydrogen and helium atoms are completely ionized ($x_{\rm HI}=0$, $x_{\rm HII}=1$, $x_{\rm HeI}=0$), $x_{\rm HeII}=1-x_{\rm HeIII}$ that means $x_{\rm e}=1+f_{\rm He}(1+x_{\rm HeIII})$ and above equation can be easily solved for $x_{\rm e}$. It proves that already at $z\sim5000$ all helium atoms become singly ionized. This holds up to $z\sim3500$ when HeI begins to recombine. At this stage $t_{\rm Hubble}:t_{\rm T}:t_{\rm HI}:t_{\rm HeI}\simeq1:0.0000003:0.0003:0.001$ and conditions are close to LTE. Until the part of HeI constitutes less than 1% of

total helium content the metastable 2s level plays insignificant role in deviation of radiative recombination rate of HeI from LTE one and ionized fraction $x_{\rm HII}$ is described yet enough accurately by Saha equation

$$\frac{x_{\rm e}x_{\rm HeII}}{x_{\rm HeI}} = 4\frac{(2\pi m_{\rm e}kT_m)^{3/2}}{h^3n_{\rm H}} e^{-\chi_{\rm HeI}/kT_m}.$$
 (2)

Now $x_{\rm HeIII} = 0$ and $x_{\rm HeI} = 1 - x_{\rm HeII}$. To run an accurate calculation of $x_{\rm HeII}$ we have to obtain the exact value of $x_{\rm e} = x_{\rm HII} + f_{\rm He}x_{\rm HeII}$. Approximation $x_{\rm HII} = 1$ is already too rough since 0.1%-decreasing of $n_{\rm HII}$ due to hydrogen recombination results in comparable change of $n_{\rm e}$ from HeI recombination because of the prevalent content of hydrogen ($f_{\rm H} = n_{\rm H}/(n_{\rm H} + n_{\rm He}) = 0.921$). So, hydrogen recombination must be taken into account too. At this stage it is described by Saha equation:

$$\frac{x_{e}x_{HII}}{x_{HI}} = \frac{(2\pi m_{e}kT_{m})^{3/2}}{h^{3}n_{H}} e^{-\chi_{HI}/kT_{m}}.$$
(3)

The system of these two equations can be reduced to cubic algebraic equation for x_e which has one real root:

$$x_{\rm e} = 2\sqrt{-A/3}\cos\left(\alpha/3\right) - B/3,\tag{4}$$

where $B = R_{\rm HI} + R_{\rm HeI}$, $R_{\rm HeI}$ and $R_{\rm HI}$ are right-hand parts of equations (2) and (3), $\cos \alpha = C/2\sqrt{-A^3/27}$, $A = D - B^2/3$, $D = R_{\rm HI}R_{\rm HeI} - R_{\rm HI} - f_{\rm He}R_{\rm HeI}$, $C = 2B^3/27 - BD/3 - E$, $E = -R_{\rm HI}R_{\rm HeI}(1 - f_{\rm He})$. I have complemented the code RECFAST by this solution to achieve correct solution of task formulated above on number density perturbations of ions. However, it does not affect the results of calculations for x's noticeably.

However, such simple description of joint hydrogen-helium recombination loses accuracy very soon, at $z \approx 2800$. Primarily the recombination becomes unequilibrium for HeI because particularity of radiative atomic processes in the expanding cooling Universe. Both recombination to the ground state and photoionization from it can be omitted because any recombination directly to the ground state will emit a photon with energy greater than potential of ionization and it will immediately ionize a neighbouring atom. So, the case B recombination takes place for HeII as well as for HII. Excited atoms of $n \geq 2$ states are ionized by photons of lower energy, belonging to continua of the second and following series, where the number density of photons is larger than one of the basic series. Therefore the entire recombination process of HeI slows down. The cool radiation field which is very strong causes the "bottleneck" effect (for details see Seager et al. (2000)) creating the overpopulation of excited states relatively to the Boltzmann distribution. So, the Saha equation does not describe adequately the recombination more and equations of detailed balance must be utilized. In the effective three-level atom approximation they lead to a single differential equation for the ionization fraction of HeII (Seager et al. 1999):

$$\frac{dx_{\rm HeII}}{dz} = \frac{x_{\rm HeII}x_{\rm e}n_{\rm H}\alpha_{\rm HeII} - \beta_{\rm HeI}(1 - x_{\rm HeII})e^{-h\nu_{\rm HeI2}1_{\rm s}/kT_{\rm m}}}{H(z)(1 + z)} \frac{1 + K_{\rm HeI}\Lambda_{\rm He}n_{\rm H}(1 - x_{\rm HeII})e^{-h\nu_{ps}/kT_{\rm m}}}{1 + K_{\rm HeI}(\Lambda_{\rm He} + \beta_{\rm HeI})n_{\rm H}(1 - x_{\rm HeII})e^{-h\nu_{ps}/kT_{\rm m}}} ,$$
(5)

where

$$\alpha_{\text{HeI}} = q \left[\sqrt{\frac{T_{\text{m}}}{T_2}} \left(1 + \sqrt{\frac{T_{\text{m}}}{T_2}} \right)^{1-p} \left(1 + \sqrt{\frac{T_{\text{m}}}{T_1}} \right)^{1+p} \right]^{-1}$$
(6)

is effective recombination coefficient (m³s⁻¹) of HeI (Hummer & Storey 1998), β_{HeI} – photoionization coefficient, $K_{\text{HeI}} \equiv \lambda_{\text{HeI2}^1p}^3/[8\pi H(z)]$ – factor which takes into account the cosmological redshifting of HeI 2^1p-1^1s photons. The values for the rest of parameters included into the right-hand part of equation (6) are listed in Table A1. Like in the previous case the rate equation for HeI recombination ought to be integrated jointly with equation for HI recombination. Until n_{HI} is still lesser than 1% of n_{H} the hydrogen ionization fraction, x_{HII} , it can be calculated enough accurate using the Saha equation (1600 $\leq z \leq 2800$). Optical depth for Ly α emission increases with growth of number of hydrogen atoms in the ground state. Diffuse Ly α photons, two-photon absorption and collisions as well as cascade recombination from upper levels result in overpopulation of the first excited level. Instantaneous spontaneous transition 2p-1s originates Ly α photon which is reabsorbed immediately by neighbouring HI atoms in the ground state and distribution of levels populations remains unchanged (case B recombination). The metastable state 2s of HI is very important for the recombination kinetics because at these redshifts the probability of two-photon 2s-1s transition is much smaller than one of photoionization. Therefore, hydrogen atoms can be ionized from the first excited state by photons of Balmer continuum, the number density in which exceeds the one of Lyman continuum. Jointly with the overpopulation of upper levels relative to a Boltzmann distribution in the strong cool radiation field (the "bottleneck" effect Seager et al. (2000)) it leads to non-equilibrium kinetics of recombination. In this case the equation of detailed balance must be used to find hydrogen ionization fraction (Peebles 1968; Seager et al. 1999):

$$\frac{dx_{\rm HII}}{dz} = \frac{x_{\rm e}x_{\rm HII}n_{\rm H}\alpha_{\rm H} - \beta_{\rm H}(1 - x_{\rm HII})e^{-h\nu_{\rm H2s}/kT_{\rm m}}}{H(z)(1 + z)} \frac{1 + K_{\rm H}\Lambda_{\rm H}n_{\rm H}(1 - x_{\rm HII})}{1 + K_{\rm H}(\Lambda_{\rm H} + \beta_{\rm H})n_{\rm H}(1 - x_{\rm HII})},$$
(7)

where

$$\alpha_{\rm H} = F \cdot 10^{-19} a t^b / (1 + c t^d) \, \text{m}^3 \text{s}^{-1}$$
 (8)

hydrogen recombination coefficient (Péquignot et al. 1991), $t = T_m/10^4$, $K_{\rm H} \equiv \lambda_{\rm H2p}^3/[8\pi H(z)]$ - factor which take into account

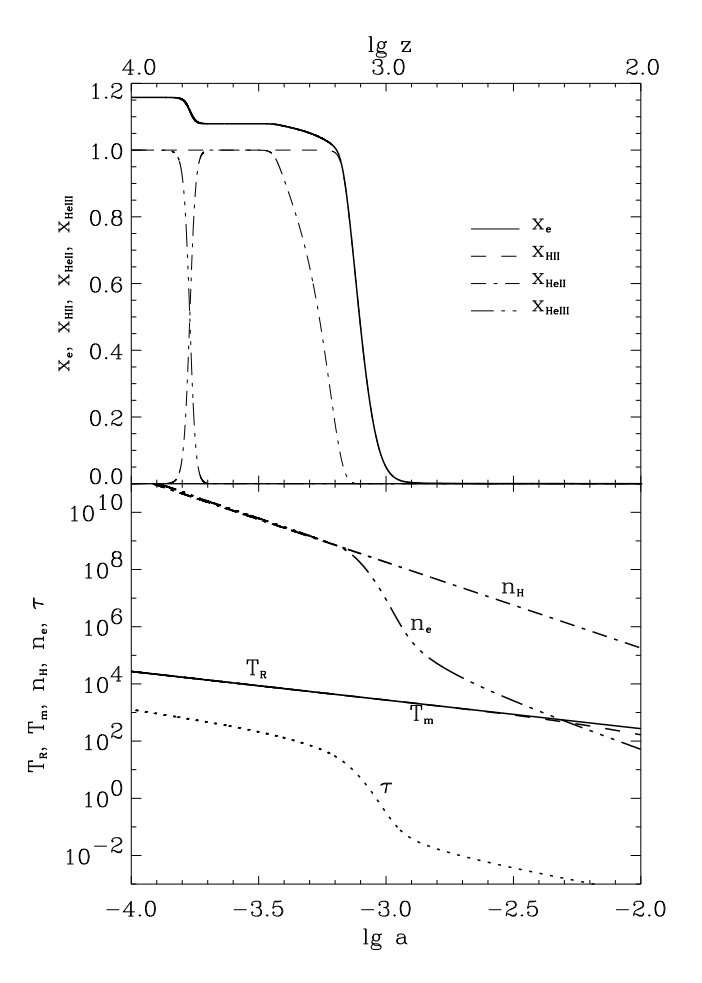


Figure 1. Hydrogen and helium recombination in Λ CDM model ($\Omega_b = 0.05$, $\Omega_{\text{CDM}} = 0.3$, $\Omega_{\Lambda} = 0.65$, h = 0.65) (top panel). The dependences of radiation temperature T_{R} (K), matter temperature T_m (K), total hydrogen number density n_{H} (m⁻³), number density of electrons n_{e} (m⁻³) and Thomson scattering optical depth $\tau = \int_0^a c\sigma_{\text{T}} n_{\text{e}} H^{-1} d \ln a$ on scale factor $a = (z+1)^{-1}$ (bottom panel).

cosmological redshifting of Ly α photons. Values for rest of parameters are presented in Table A1. Photoionization coefficients in (5) and (7) are calculated via the case B recombination coefficients in the following way:

$$\beta = \alpha (2\pi m_{\rm e} k T_{\rm m}/h^2)^{3/2} e^{-h\nu_{2s-1s}/kT_{\rm m}}.$$
(9)

The temperature of electrons and ions, $T_{\rm m}$, practically coincides with radiation temperature, $T_{\rm R}$, in the range before $z \sim 800$, since until this moment the time-scale of Thomson scattering remains essentially lower than the time-scale of Universe expansion, $t_{\rm T}/t_{\rm Hubble} < 10^{-3}$. Therefore, until this moment the rate of temperature decreasing is governed by adiabatic cooling of radiation ($\gamma = 4/3$) caused by Universe expansion:

$$\frac{dT_{\rm m}}{dz} = \frac{T_{\rm m}}{(1+z)}.\tag{10}$$

After recombination, at z < 800, adiabatic cooling of ideal gas ($\gamma = 5/3$) begins to dominate over the heating caused by Compton effect which is a main process of energy transfer between electrons and photons. Cooling of plasma via free-free, free-bound and bound-bound transitions and collisional ionization as well as heating via photoionization and collisional recombination gives insignificant contribution into the rate of temperature change, it does not exceed the 0.01% of main processes – adiabatic cooling and heating by Compton effect (Seager et al. 2000). So, at this epoch the following equation for the rate of temperature change proves to be enough accurate (Weymann 1965; Peebles 1968; Seager et al. 1999):

$$\frac{dT_{\rm m}}{dz} = \frac{8\sigma_{\rm T} a_{\rm R} T_{\rm R}^4}{3H(z)(1+z)m_{\rm e}c} \frac{x_{\rm e}(T_{\rm m} - T_{\rm R})}{1+f_{\rm He} + x_{\rm e}} + \frac{2T_{\rm m}}{(1+z)},\tag{11}$$

The Table A1 lists the values of all atomic constants and coefficients of approximation formulae seen in equations (1)-(11).

The results of calculations of ionization history in the Λ CDM model of the Universe, performed on the base of equations (1)-(11) and RECFAST code complemented by solution (4), are presented in Fig.1. There are also shown the dependences of radiation temperature $T_{\rm R}$, matter temperature $T_{\rm m}$, number density of hydrogen nuclei $n_{\rm H}$, number density of electrons $n_{\rm e}$ and optical depth τ due to Thomson scattering by electrons $\tau(z) = \int_0^z c\sigma_{\rm T} n_{\rm e}(z) H^{-1}(z)(z+1)^{-1} dz$ on redshift z (top abscissa axis in figure). In consequence of rapid expansion of the Universe and non-equilibrium kinetics of recombination-ionisation

processes the hydrogen and helium recombinations do not finish with absolutely neutral medium and some ionized fractions persist at low redshifts that is called the residual ionization. The calculations show that at $z=200~x_{\rm e}\approx x_{\rm HII}=6.7\cdot10^{-4}$ (Fig.1), $x_{\rm HeII}=9.2\cdot10^{-10}$ and at $z=0~x_{\rm e}\approx x_{\rm HII}=4.1\cdot10^{-4}$, $x_{\rm HeII}=8.1\cdot10^{-10}$ (an emergence of hydrogen molecules H₂, H₂⁺ and negative hydrogen ions, H⁻, does not change these values essentially since their number densities are of several orders lower than free electrons ones (Seager et al. 2000)). Residual values of ions fractions decrease with increasing of total baryon content. In fact, if $\Omega_b=0.06$ then at $z=200~x_{\rm e}\approx x_{\rm HII}=6.3\cdot10^{-4}$, $x_{\rm HeII}=2.0\cdot10^{-10}$. Stronger dependence of residual values of helium ionized fraction (HeII) on baryon content when compared to the hydrogen one (HII) is explained by different atomic structures of HI and HeI atoms and conditions under which these recombinations occur: helium due to its higher potential of ionization starts to recombine earlier when number densities of plasma particles are higher and its recombination proceed in the conditions of high number density of free electrons caused by the complete hydrogen ionization.

2 PERTURBATIONS OF NUMBER DENSITIES OF IONS AND ELECTRONS

2.1 Definitions

Let the values of ionization fractions of HI, HII, HeII, HeII, HeIII and electrons averaged over the whole space at fixed cosmological time be x_i , where "i" marks each component among them. Let us denote as \hat{x}_i the local value of relative number density of each component in the range of cosmological density perturbation of baryonic matter $\delta_b \equiv \delta \rho_b/\rho_b \ll 1$, were ρ_b is its matter density. Its deviation from mean value we mark as δx_i , so that $\hat{x}_i = x_i + \delta x_i$ and δx_i is called the perturbation of relative number density of *i*-th component. Relative perturbations of relative number densities of ions and free electrons we define as $\Delta_i \equiv \delta x_i/x_i$. It is obvious that $\Delta_e = \delta n_e/n_e - \delta n_H/n_H$, $\Delta_{HII} = \delta n_{HII}/n_{HII} - \delta n_H/n_H$, $\Delta_{HeII} = \delta n_{HeII}/n_{HeII} - \delta n_{He}/n_{He}$. We suppose that primordial chemical composition of baryon matter is uniform (f_{He} is constant), so $\delta n_H/n_H = \delta n_{He}/n_{He} = \delta_b$ and

$$\Delta_i = \delta_i - \delta_b,\tag{12}$$

where $\delta_i \equiv \delta n_i/n_i = \Delta_i + \delta_b$ is relative number density perturbation of *i*-th component. It must be noted, that in expanding universe the recombination does not end with the completely neutral hydrogen or helium, but with residual ionization (see last paragraph of previous section). Therefore, none of values n_i does reach zero and ambiguity of "0/0"-type in δ_i does not appear. So, Δ_i 's do not take diverging values ever as it seen from (12). Numerical results presented below prove that.

Therefore, Δ_i is difference of two relative perturbations: of number density of "i"-th component and density of all baryonic matter. Since δ_i and δ_b are scalar functions of four coordinates in some gauge, so under the gauge transformations which do not change the cosmological background characteristics (mean CMB temperature, isotropic Hubble expansion etc.) each from them is transformed by adding the same expression from component of transformation of time coordinate (see for details Bardeen (1980); Kodama & Sasaki (1984); Durrer (2001)). Whereas in (12) they appear with opposite signs then Δ_i 's keep unchanged under such transformations, so they are gauge-invariant quantities.

If ionization degree does not change with time, that is valid when hydrogen or helium are entirely ionized, then $\delta_i = \delta_b$ and $\Delta_i = 0$. If the photorecombination and photoionization rates as well as ionization degree of some component change, then δ_i and δ_b can vary with different rates because the altering of δ_b is driven by gravitation and stress of baryon-photon plasma, while δ_i is additionally influenced by kinetics of ionization-recombination processes. Therefore, Δ_i is measure of deviation of relative number density perturbations of "i"-th component from relative density perturbation of total baryon component as a result of changing of recombination and ionization rates within cosmological density perturbation.

At enough early stage of evolution of the Universe for adiabatic density perturbations of scales larger than the horizon $\delta_m = \delta_b$ and relative perturbations of radiation energy density $\delta_R \equiv \delta \epsilon_R / \epsilon_R = 4 \delta_b / 3$. Since $\epsilon_R = a T_R^4$, then $\delta_{T_R} \equiv \delta T_R / T_R = 1/3 \delta_b$. For isothermal perturbations $\delta_{T_R} = 0$.

2.2 Equations

Long before and much after recombination the local baryon mass density fluctuations most probably lead to corresponding perturbations of number densities of ions and electrons, $\delta_i \approx \delta_b$. But at the recombination epoch because of dependence of ionization-recombination process rates on density and temperature of baryon matter the distribution of atoms over ionization stages within those perturbations will somewhat depart from background one and $\Delta_i \neq 0$ is expected to be true. We study the cosmological perturbations of small amplitudes, so the ratio $t_{\text{Hubble}}: t_{\text{T}}: t_{\text{HI}}: t_{\text{HeI}}$ remains practically the same as for background. It means that within cosmological perturbations the same equations (1)-(11) are applicable and connection between the perturbations of ion number density and cosmological perturbations of density and temperature may be obtained by variation of those equations.

Varying the variables $n_{\rm H}$, T_m , $x_{\rm HeII}$, $x_{\rm HeIII}$ and x_e in the equation (1) we will obtain:

$$\Delta_{\text{HeIII}} = \frac{x_{\text{e}}(1 - x_{\text{HeIII}})}{x_{\text{e}} + (1 - x_{\text{HeIII}})x_{\text{HeIII}}f_{\text{He}}} \left[\left(\frac{3}{2} + \frac{\chi_{\text{HeII}}}{kT_m} \right) \delta_{T_m} - \delta_b \right], \quad \Delta_{\text{HeII}} = -\Delta_{\text{HeIII}}, \quad \Delta_{\text{e}} = \frac{x_{\text{HeIII}}}{x_{\text{e}}} f_{\text{He}} \Delta_{\text{HeIII}}, \quad (13)$$

Here it is assumed that $x_{\rm HI} = x_{\rm HeI} = 0$ at z > 3500 and relative perturbations of rest of components have vanished too. One can see that relative perturbations of relative number densities of ions HeIII is the linear combination of cosmological

perturbations of temperature and mass density of baryon matter. Within an adiabatic perturbation $\Delta_{\rm HeIII}$ has the same sign as temperature fluctuation and opposite to mass density one. The values of $x_{\rm e}$ and $x_{\rm HeIII}$ are calculated from (1). The asymptotical behaviour of $\Delta_{\rm HeIII}$ follows from (13): at z > 7000 when $x_{\rm HeIII} \to 1$ (all helium atoms become double ionized) $\Delta_{\rm HeIII} \to 0$ ($\delta_{\rm HeIII} = \delta_b$). On the other hand, at z < 5000 when $x_{\rm HeIII} \to 0$ $\Delta_{\rm HeIII} \to \frac{X_{\rm HeII}}{kT_m} \delta_{T_m}$ and increases with temperature decreasing. It is obvious that the second asymptotics is not physically correct. Indeed, such monotonous increasing of $\Delta_{\rm HeIII}$ is caused by vanishing of $x_{\rm HeIII}$ (see Fig.1) and does not describe the real number density perturbation of HeIII ions. That is why in Fig.2 in the range of 5000 < z < 7000 the absolute values of perturbations of number density $\delta x_{\rm HeIII}$ and $\delta x_{\rm HeIII}$ are presented.

At 3500 < z < 5000 both hydrogen and helium are entirely ionized: $x_{\rm HII} = x_{\rm HeII} = 1$, $x_{\rm HI} = x_{\rm HeII} = x_{\rm HeII} = 0$. So, at this period the amplitudes of all relative perturbations equal to zero. With subsequent decreasing of temperature the HeI atoms and afterwards HI ones begin to recombine. The kinetics of their recombination is described by Saha equations (2) and (3). Variation of these equations gives the following expressions for relative perturbations of relative number density of helium $\Delta_{\rm HeII}$, hydrogen $\Delta_{\rm HII}$ and free electrons $\Delta_{\rm e}$:

$$\Delta_{\text{HeII}} = (1 - x_{\text{HeII}}) \frac{(1 - x_{\text{HII}}) x_{\text{HII}} \left(\frac{x_{\text{HI}}}{k T_m} - \frac{x_{\text{HeI}}}{k T_m}\right) \delta_{\text{T}_m} + x_{\text{e}} \left[\left(\frac{3}{2} + \frac{x_{\text{HeI}}}{k T_m}\right) \delta_{\text{T}_m} - \delta_b\right]}{(1 - x_{\text{HII}}) x_{\text{HII}} + (1 - x_{\text{HeII}}) x_{\text{HeII}} f_{\text{He}} - x_{\text{e}}},$$
(14)

$$\Delta_{\rm HII} = \frac{(1 - x_{\rm HII})x_{\rm e} \left[\left(\frac{3}{2} + \frac{X_{\rm HI}}{kT_m} \right) \delta_{\rm T_m} - \delta_b \right]}{(1 - x_{\rm HII})x_{\rm HII} + (1 - x_{\rm HeII})x_{\rm HeII}f_{\rm He} - x_{\rm e}},\tag{15}$$

$$\Delta_{e} = \frac{(1 - x_{\text{HII}})x_{\text{HII}} \frac{\chi_{\text{HII}}}{kT_{m}} (1 + (1 - x_{\text{HeII}})x_{\text{HeII}}/x_{e})}{(1 - x_{\text{HII}})x_{\text{HII}} + (1 - x_{\text{HeII}})x_{\text{HeII}}f_{\text{He}} - x_{e}} \delta_{\text{T}_{m}} + \frac{(1 - x_{\text{HeII}})x_{\text{HeII}}\frac{\chi_{\text{HeII}}}{kT_{m}} (f_{\text{He}} - (1 - x_{\text{HII}})x_{\text{HIII}}/x_{e})}{(1 - x_{\text{HII}})x_{\text{HII}} + (1 - x_{\text{HeII}})x_{\text{HeII}}f_{\text{He}} - x_{e}} \delta_{\text{T}_{m}} + \frac{(1 - x_{\text{HIII}})x_{\text{HIII}} + (1 - x_{\text{HeII}})x_{\text{HeII}}f_{\text{He}} - x_{e}}{(1 - x_{\text{HIII}})x_{\text{HIII}} + (1 - x_{\text{HeII}})x_{\text{HeII}}f_{\text{He}}} \left[\frac{3}{2}\delta_{\text{T}_{m}} - \delta_{b}\right]$$

$$(16)$$

Their asymptotic behaviour for $x_{\rm HeII} \to 1$ and $x_{\rm HII} \to 1$ agrees with our anticipations and appears to be the same as for $\Delta_{\rm HeII}$ case: $\Delta_{\rm HeII}$, $\Delta_{\rm HII}$ and $\Delta_{\rm e} \to 0$. Other asymptotics for $x_{\rm HeII} \to 0$ and $x_{\rm HII} \to 0$ have not physical sense, since for $x_{\rm HeII} \leqslant 0.99$ and $x_{\rm HII} \leqslant 0.99$ it is necessary to use the non-equilibrium rate equations and energy balance (5)-(11). In this case the differential equations for relative perturbations $\Delta_{\rm HII}$, $\Delta_{\rm HeII}$ and $\delta_{\rm T_m}$ are obtained by variation of (5)-(11):

$$x_{\text{HeII}} \frac{d\Delta_{\text{HeII}}}{dz} = \frac{\left(1 + K_{\text{HeI}}\Lambda_{\text{He}}n_{\text{H}}(1 - x_{\text{HeII}})e^{-h\nu_{ps}/kT_{\text{m}}}\right) x_{\text{HeII}}x_{\text{e}}n_{\text{H}}\alpha_{\text{HeII}}}{H(z)(1 + z) \left(1 + K_{\text{HeI}}(\Lambda_{\text{He}} + \beta_{\text{HeI}})n_{\text{H}}(1 - x_{\text{HeII}})e^{-h\nu_{ps}/kT_{\text{m}}}\right) \left[\Delta_{\text{e}} + \Delta_{\text{HeII}} + \delta_{b} + \frac{\delta\alpha_{\text{HeII}}}{\alpha_{\text{HeII}}}\right] - \frac{\left(1 + K_{\text{HeI}}\Lambda_{\text{He}}n_{\text{H}}(1 - x_{\text{HeII}})e^{-h\nu_{ps}/kT_{\text{m}}}\right) \beta_{\text{HeI}}(1 - x_{\text{HeII}})e^{-h\nu_{ps}/kT_{\text{m}}}}{H(z)(1 + z) \left(1 + K_{\text{HeI}}(\Lambda_{\text{He}} + \beta_{\text{HeI}})n_{\text{H}}(1 - x_{\text{HeII}})e^{-h\nu_{ps}/kT_{\text{m}}}\right) \left[\frac{\delta\beta_{\text{HeI}}}{\beta_{\text{HeI}}} - \frac{x_{\text{HeII}}}{1 - x_{\text{HeII}}}\Delta_{\text{HeII}} + \frac{h\nu_{\text{HeII}}^{2}}{kT_{\text{m}}}\delta_{T_{\text{m}}}\right] + \frac{dx_{\text{HeII}}}{dz} \frac{K_{\text{HeI}}\Lambda_{\text{He}}n_{\text{H}}(1 - x_{\text{HeII}})e^{-h\nu_{ps}/kT_{\text{m}}}}{1 + K_{\text{HeI}}\Lambda_{\text{He}}n_{\text{H}}(1 - x_{\text{HeII}})e^{-h\nu_{ps}/kT_{\text{m}}}} \left[\delta_{b} - \frac{x_{\text{HII}}}{1 - x_{\text{HII}}}\Delta_{\text{HeII}} + \frac{h\nu_{ps}}{kT_{\text{m}}}\delta_{T_{\text{m}}}\right] - \Delta_{\text{HeII}} \frac{dx_{\text{HeII}}}{dz} - \frac{dx_{\text{HeII}}}{1 - x_{\text{HeII}}}\frac{\delta\beta_{\text{HeI}}}{dz} - \frac{dx_{\text{HeII}}}{1 - x_{\text{HeII}}}\frac{\delta\beta_{\text{HeI}}}{dz} - \frac{\delta\beta_{\text{HeI}}}{\Lambda_{\text{He}} + \beta_{\text{HeI}}}\frac{\delta\beta_{\text{HeI}}}{\beta_{\text{HeI}}}\right],$$

$$-\frac{dx_{\text{HeII}}}{dz} \frac{K_{\text{HeI}}(\Lambda_{\text{He}} + \beta_{\text{HeI}})n_{\text{H}}(1 - x_{\text{HeII}})e^{-h\nu_{ps}/kT_{\text{m}}}}{1 - x_{\text{HIII}}}\Delta_{\text{HeII}} + \frac{h\nu_{ps}}{kT_{\text{m}}}\delta_{T_{\text{m}}} + \frac{\beta_{\text{HeI}}}{\Lambda_{\text{He}} + \beta_{\text{HeI}}}\frac{\delta\beta_{\text{HeI}}}{\beta_{\text{HeI}}}}\right],$$

$$-\frac{dx_{\text{HeII}}}{dz} \frac{K_{\text{HeI}}(\Lambda_{\text{He}} + \beta_{\text{HeI}})n_{\text{H}}(1 - x_{\text{HeII}})e^{-h\nu_{ps}/kT_{\text{m}}}}{1 - x_{\text{HIII}}}\Delta_{\text{HeII}} + \frac{h\nu_{ps}}{kT_{\text{m}}}\delta_{T_{\text{m}}} + \frac{\beta_{\text{HeI}}}{\Lambda_{\text{He}} + \beta_{\text{HeI}}}\frac{\delta\beta_{\text{HeI}}}{\beta_{\text{HeI}}}}\right],$$

$$-\frac{dx_{\text{HeII}}}{dz} \frac{K_{\text{HeI}}(\Lambda_{\text{He}} + \beta_{\text{HeI}})n_{\text{H}}(1 - x_{\text{HeII}})e^{-h\nu_{ps}/kT_{\text{m}}}}}{1 - x_{\text{HeII}}}e^{-h\nu_{ps}/kT_{\text{m}}}}\left[\delta_{\text{heII}} - \frac{\lambda_{\text{HeII}}}{\lambda_{\text{HeII}}} + \frac{\lambda_{\text{HeII}}}{\lambda_{\text{HeII}}} + \frac{\lambda_{\text{HeII}}}{\lambda_{\text{HeII}}}e^{-h\nu_{\text{HeII}}}\frac{\delta\beta_{\text{HeII}}}{\lambda_{\text{HeII}}}\right],$$

$$-\frac{dx_{\text{HeII}}}{dz} \frac{\lambda_{\text{HeII}}}{1 - x_{\text{HeII}}}e^{-h\nu_{\text{HeII}}}e^{-h\nu_{\text{HeII}}}e^{-h\nu_{\text{HeII}}}e^{-h\nu_{\text{HeII}}}e^{$$

$$x_{\text{HII}} \frac{d\Delta_{\text{HII}}}{dz} = \frac{(1 + K_{\text{HI}}\Lambda_{\text{H}}n_{\text{H}}(1 - x_{\text{HII}})) x_{\text{HII}}x_{\text{e}}n_{\text{H}}\alpha_{\text{HII}}}{H(z)(1 + z) (1 + K_{\text{HI}}(\Lambda_{\text{H}} + \beta_{\text{HI}})n_{\text{H}}(1 - x_{\text{HII}}))} \left[\Delta_{\text{e}} + \Delta_{\text{HII}} + \delta_{b} + \frac{\delta\alpha_{\text{HI}}}{\alpha_{\text{HI}}} \right] + \\ + \frac{(1 + K_{\text{HI}}\Lambda_{\text{H}}n_{\text{H}}(1 - x_{\text{HII}})) \beta_{\text{HI}}(1 - x_{\text{HII}})e^{-h\nu_{\text{H}2s}/kT_{\text{m}}}}{H(z)(1 + z) (1 + K_{\text{HI}}(\Lambda_{\text{H}} + \beta_{\text{HI}})n_{\text{H}}(1 - x_{\text{HII}})} \left[\frac{\delta\beta_{\text{HI}}}{\beta_{\text{HI}}} - \frac{x_{\text{HII}}}{1 - x_{\text{HII}}} \Delta_{\text{HII}} + \frac{h\nu_{\text{H}2s}}{kT_{\text{m}}} \delta_{T_{\text{m}}} \right] + \\ + \frac{dx_{\text{HII}}}{dz} \frac{K_{\text{HI}}\Lambda_{\text{H}}n_{\text{H}}(1 - x_{\text{HII}})}{1 + K_{\text{HI}}\Lambda_{\text{H}}n_{\text{H}}(1 - x_{\text{HII}})} \left[\delta_{b} - \frac{x_{\text{HII}}}{1 - x_{\text{HII}}} \Delta_{\text{HII}} \right] - \Delta_{\text{HII}} \frac{dx_{\text{HII}}}{dz} - \\ - \frac{dx_{\text{HII}}}{dz} \frac{K_{\text{HI}}(\Lambda_{\text{H}} + \beta_{\text{HI}})n_{\text{H}}(1 - x_{\text{HII}})}{1 + K_{\text{HI}}(\Lambda_{\text{H}} + \beta_{\text{HI}})n_{\text{H}}(1 - x_{\text{HII}})} \left[\delta_{b} - \frac{x_{\text{HII}}}{1 - x_{\text{HII}}} \Delta_{\text{HII}} + \frac{\beta_{\text{HI}}}{\Lambda_{\text{H}} + \beta_{\text{HI}}} \frac{\delta\beta_{\text{HI}}}{\beta_{\text{HI}}} \right],$$

$$(18)$$

$$T_{\rm m} \frac{d\delta_{T_{\rm m}}}{dz} = \frac{8\sigma_{\rm T} a_{\rm R} T_{\rm R}^4}{3H(z)(1+z)m_{\rm e}c} \frac{x_{\rm e}}{1+f_{\rm He}+x_{\rm e}} \left[4(T_{\rm m}-T_{\rm R})\delta_{T_{\rm m}} + \frac{1+f_{\rm He}}{1+f_{\rm He}+x_{\rm e}} (T_{\rm m}-T_{\rm R})\Delta_{\rm e} + T_{\rm m}\delta_{T_{\rm m}} - T_{\rm R}\delta_{T_{\rm R}} \right] + \frac{2T_{\rm m}}{1+z}\delta_{T_{\rm m}} - \frac{dT_{\rm m}}{dz}\delta_{T_{\rm m}},$$
(19)

where $\frac{dx_{\text{HeII}}}{dz}$, $\frac{dx_{\text{HII}}}{dz}$ and $\frac{dT_{\text{m}}}{dz}$ mean the same as the right-hand side of (5), (7) and (11) respectively. The variations of recombination coefficients are expressed via temperature perturbations by the equations:

$$\frac{\delta \alpha_{\rm HI}}{\alpha_{\rm HI}} = \left(b - \frac{d \cdot c \cdot t^d}{1 + c \cdot t^d}\right) \delta_{T_{\rm m}},$$

$$\frac{\delta \alpha_{\rm HeI}}{\alpha_{\rm HeI}} = -\frac{1}{2} \left(1 + \frac{(1-p)\sqrt{T_{\rm m}/T_2}}{1 + \sqrt{T_{\rm m}/T_2}} + \frac{(1+p)\sqrt{T_{\rm m}/T_1}}{1 + \sqrt{T_{\rm m}/T_1}} \right) \delta_{T_{\rm m}},$$

Then the variations of photoionization rates can be calculated in the following way:

$$\frac{\delta \beta_i}{\beta_i} = \frac{\delta \alpha_i}{\alpha_i} + \frac{3}{2} \delta_{T_{\rm m}} + \frac{h \nu_{i2s}}{k T_{\rm m}} \delta_{T_{\rm m}}.$$

So, equations (17)-(19) constitute the system of three ordinary linear differential equations of first order for relative perturbations of ions and electrons relative number densities and matter temperature, which can be solved using the publicly available code DVERK¹. The initial data for them are equilibrium values of relative perturbations of ion relative number density at the moment when $x_{\rm HII} > 0.99$ and $x_{\rm HeII} > 0.99$ calculated by (14)-(15).

Let us use the equations (13)-(19) to analyse the evolution of relative ion density perturbations and temperature of baryonic matter. Since all these equations have solutions in unperturbed problem therefore it seems naturally to supplement the code RECFAST (Seager et al. 1999) with block for calculation of perturbations of ionized fractions. The complemented code $drecfast.f^2$ is used further in our analysis of perturbations of ion number density and matter temperature.

2.3 Results

To estimate the magnitude of probable effect it is useful first to consider the stationary adiabatic mass density perturbation of baryon matter with some amplitude. Its spatial shape does not matter for our analysis. One may assume for simplicity that it is homogeneous in some region of space.

The results of calculations of ion number density relative perturbations (13)-(19) caused by adiabatic positive matter density perturbation (overdensity) with $\delta_b = 10^{-4}$ and $\delta_{T_R} = \delta_b/3$ as well as isothermal ($\delta_b = 10^{-4}$, $\delta_{T_R} = 0$) and "thermal" ($\delta_b = 0$, $\delta_{T_R} = \frac{1}{3} \cdot 10^{-4}$) ones are presented in Fig.2 for the range of redshifts 200 < z < 10000. One can see that the appreciable deviations of relative perturbations of ion number density $\Delta_{\rm HII}$, $\Delta_{\rm HeII}$ and $\Delta_{\rm e}$ from perturbation of total baryon mass density δ_b arise in cosmological recombination epoch (800 < z < 1500) as result of amplification of photorecombination and photoionization rates. So, the amplitudes of relative perturbations of number densities of protons and electrons are of $\simeq 5$ times higher than the amplitude of total baryon number density perturbation. For helium ions HeII such ratio is even higher, $\simeq 18$. However, such large amplitude practically does not contribute to the number density perturbations of free electrons: in the Fig.2 $\Delta_{\rm HII}$ and $\Delta_{\rm e}$ are superposed in the range of 200 < z < 1500. This is because of too low number density of helium ions. Indeed, at $z \simeq 1200$, when $x_{\rm HII} \simeq 0.5$, $x_{\rm HeII} < 0.0003$. Also one can see, that relative temperature perturbations are equal to the initial ones because of dominant CMB radiation in the energy balance of recombinational plasma. So, the fluctuations in ionization-recombination rates caused by cosmological adiabatic perturbations do not result into additional noticeable local fluctuations of CMB and electron-ion temperatures.

The figures in the middle and bottom panels illustrate the role of the initial mass density perturbation and initial temperature perturbation in arising of perturbations of number densities of ions and electrons.

For the adiabatic negative (underdensity) perturbations as well as for the isothermal underdensity and cold "thermal" ones the pictures are symmetric as follows from equations (13)-(19).

3 PERTURBATIONS OF NUMBER DENSITY OF ELECTRONS IN ACDM MODEL

In previous section we have analysed the perturbations of number density of ions in the framework of "toy" model of stationary perturbations. In reality, the amplitudes of adiabatic cosmological perturbations evolve due to gravitational attraction and repulsion by stress in baryon-photon plasma in potential wells created by the density perturbations of dark matter, see for example Bardeen (1980); Kodama & Sasaki (1984); Ma & Bertschinger (1995); Hu & Sugiyama (1995); Durrer (2001) and citing therein. When the scale of perturbation becomes substantially smaller than scale of acoustic horizon (Jeans scale), then adiabatic perturbations in the baryon-photon plasma start to oscillate like the standing acoustic waves. In consequence of recombination the Jeans scale drops and the previously oscillating amplitudes of perturbations in baryon component start to monotonously increase mainly under influence of gravitational attraction of dark matter density perturbations. The amplitudes of perturbations with scale larger than acoustic horizon at recombination epoch increased $\delta_b \propto t^{1/2}$ in radiation-dominated epoch and $\delta_b \propto t^{2/3}$ after recombination in dust-like Universe. In papers (Bardeen 1980; Kodama & Sasaki 1984; Ma & Bertschinger 1995; Hu & Sugiyama 1995; Durrer 2001) one can find analytical solutions of relevant equations for evolution of relative density perturbations in simplified cases of single component mediums as well as the numerical solutions for realistic multi-component Universe.

I shall use here the numerical approach by Ma & Bertschinger (1995) and their package of FORTRAN programs COS-MICS³ in order to calculate the amplitude of baryon density perturbations in multi-component medium for synchronous gauge. The evolution of amplitudes of adiabatic density perturbations for each component of Hot plus Cold Dark Matter (HCDM)

¹ It is created by T.E. Hull, W.H.Enright, K.R. Jakson in 1976 and is available at site http://www.cs.toronto.edu/NA/dverk.f.gz

² available at http://astro.franko.lviv.ua/~novos/

³ It is available at site http://arcturus.mit.edu/cosmics/

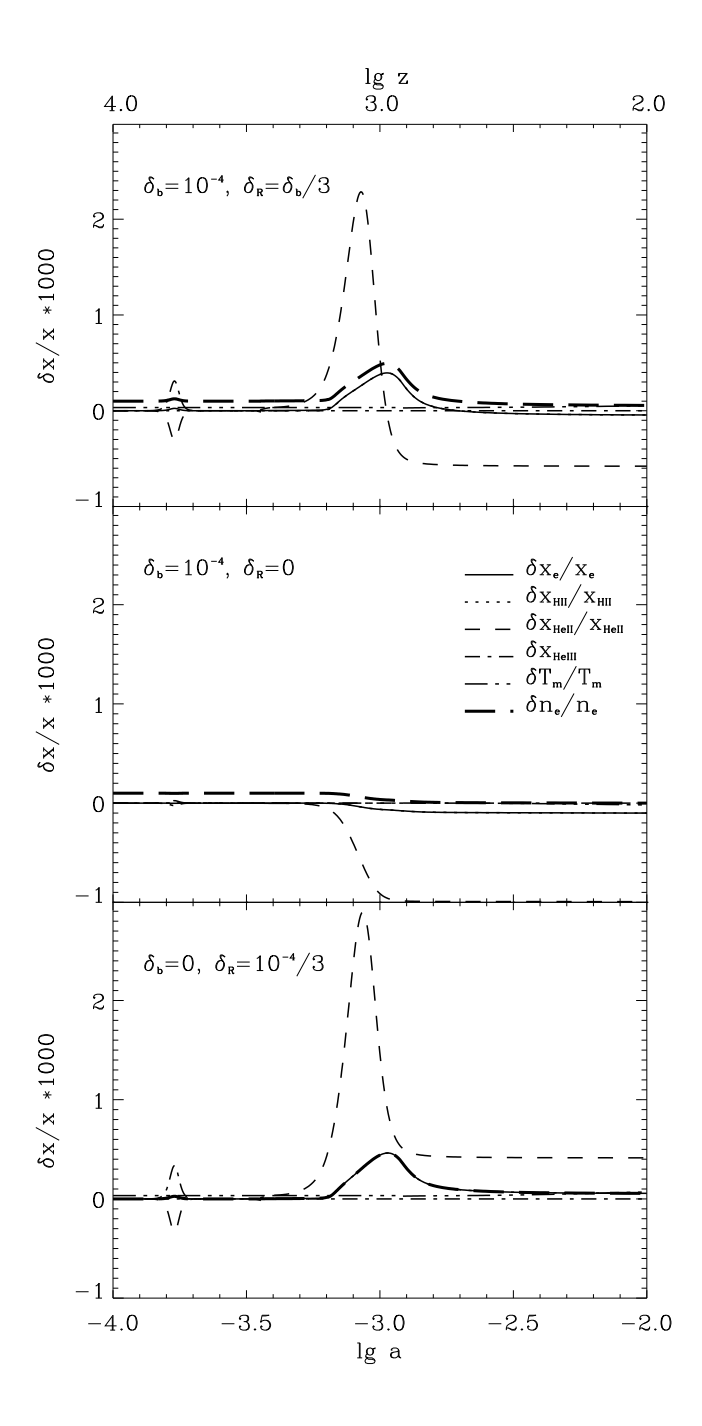


Figure 2. The relative number density perturbations of ions of helium, hydrogen and free electrons caused by adiabatic positive (overdensity) matter density initial perturbation (top panel), by isothermal perturbation (middle panel) and by hot "thermal" initial fluctuation (bottom panel).

and Λ CDM models are shown in the Fig.3. The scale of these perturbations in Fourier space is $k=0.1 \mathrm{Mpc^{-1}}$, that actually equals to the horizon distance at the epoch of radiation-matter equality and amounts approximately 1/4 of the horizon size at the decoupling epoch. So, starting from radiation-matter equality epoch $(a_{eq} \simeq 2 \cdot 10^{-4} \Omega_m h^2)$ the amplitudes of density perturbations in baryon-photon plasma oscillate acoustically till the recombination $(a_{rec} \simeq 10^{-3})$. The detailed analysis of the evolution of density perturbations of different scales in the multi-component Universe one can find in Ma & Bertschinger (1995).

In order to analyse the perturbations of number densities of ions and electrons caused by cosmological baryon density perturbations the code drecfast.f was complemented by the COSMICS' code $linger_syn.f$ as subroutine, so, that amplitude of baryon mass density perturbation δ_b and radiation temperature $\delta_{T_R} = \delta_R/4$ were precalculated at each step of integration of the equations system (13)-(19). Results of joint calculations the ion number density and mass density perturbations of different

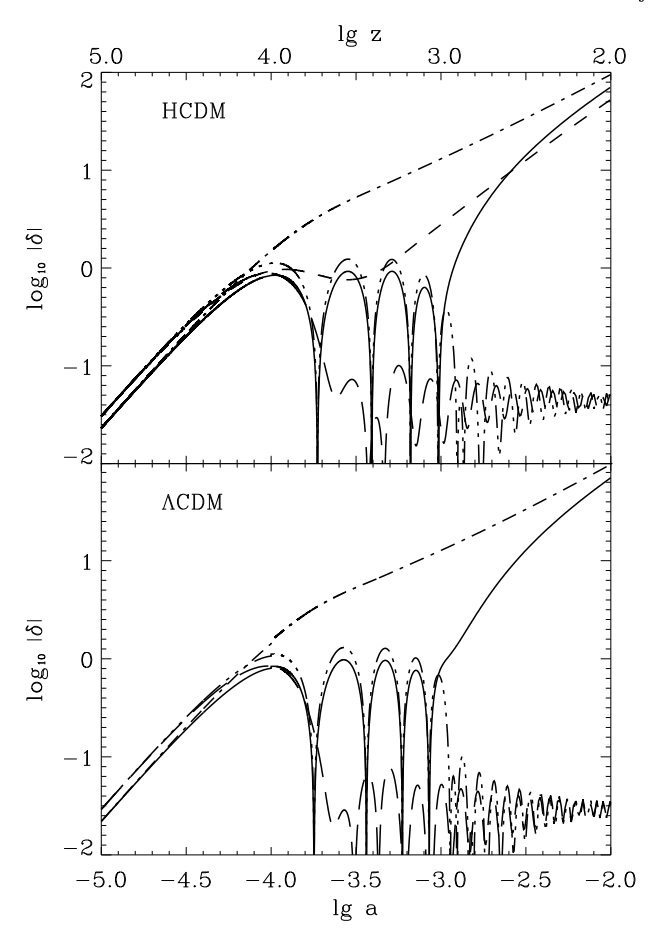


Figure 3. Evolution of amplitudes of adiabatic density perturbations for different components of HCDM ($\Omega_b = 0.05$, $\Omega_{\rm CDM} = 0.75$, $\Omega_{\nu} = 0.2$, h = 0.65) and Λ CDM ($\Omega_b = 0.05$, $\Omega_{\rm CDM} = 0.3$, $\Omega_{\Lambda} = 0.65$, h = 0.65) multi-component models in synchronous gauge as calculated by COSMICS code (arbitrary normalization). The lines represent the relative density perturbation of baryons δ_b (solid line), thermal electromagnetic radiation $\delta_{\rm R}$ (dash-three dotted line), cold dark matter δ_c (dash-dotted line), massless (long-dashed line) and massive (short-dashed line) neutrino. The scale of perturbations in Fourier space is $k = 0.1 {\rm Mpc}^{-1}$.

scales in ACDM model are presented in Fig.4. In the left-hand column the evolution of relative mass density perturbations δ_{b_1} , $\delta_{\rm R}$ and δ_{c} for the baryon, photon and CDM components (adiabatic initial conditions) are shown. Five wave numbers are plotted: $k = 0.01, 0.025, 0.05, 0.075, 0.1 \,\mathrm{Mpc^{-1}}$ (from top to bottom). In the right-hand column the perturbations of number density of electrons against baryon mass density ones are shown for the same wave numbers. In each figure the visibility function $d\tau/dze^{-\tau}$ is shown by dotted line in order to mark the position of last scattering surface. The peak of this function is found at z = 1088 and, in fact, denotes moment of decoupling of photons and baryons. The particle horizon at this moment equals $\eta_{dec} \simeq 278 \mathrm{Mpc}$ ($k_{dec} \simeq 0.023 \mathrm{Mpc}^{-1}$), sound horizon (or Jeans scale) is $\lambda_{dec}^s \simeq 160 \mathrm{Mpc}$ ($k_{dec}^s \simeq 0.039 \mathrm{Mpc}^{-1}$). Therefore, the wave numbers of particle and sound horizons at decoupling epoch fall within the range of plotted k and behaviour of baryon mass density and free electron number density perturbations of scales larger, comparable and lower in comparison with horizons are revealed. For modes with $k < 0.01 \mathrm{Mpc^{-1}}$ the relative amplitude, shape and position of peak of electron number density perturbation are the same as for $k = 0.01 \mathrm{Mpc}^{-1}$ mode. For them the peak of $\delta_{\rm e}$ is situated at $900 \le z \le 910$ and ratio of amplitudes $\delta_e/\delta_b \simeq 4.5$. For modes with $k > 0.01 {\rm Mpc}^{-1}$ the relative amplitude, shape and position of peak of electron number density perturbation vary: when a wave number increases starting from 0.01 to k_{dec}^s the peak position δ_e shifts to the position of visibility function peak with approximately the same ratio of $\delta_{\rm e}/\delta_b \approx 4.5$. For modes with $k > k_{dec}^s$ the value of $\delta_{\rm e}$ radically decreases and makes several oscillation around value of $\delta_{\rm b}$ depending on phase of $\delta_{\rm R}$ oscillation at decoupling epoch. So, ion number density fluctuations at decoupling epoch caused by recombination kinetics in the range of adiabatic density perturbations are most prominent for the large-scale perturbations with $k \leq k_{dec}^s$. At z < 800, when ionization become residual, δ_e becomes lesser than δ_b independently of scale of baryon density perturbation. The difference acquires the value $\sim 20\%$ at $z \sim 200$. It is caused by increasing of δ_b on all scales under gravitational potential of dark matter density perturbations, so, the probability of recombination is slightly higher in such regions. It is similar to the residual ionization and its inverse dependence on baryon density.

Finally it should be noted that presented results do not depend essentially on exact values of cosmological parameters of non-exotic models and are practically the same for parameters of WMAP concordance model.

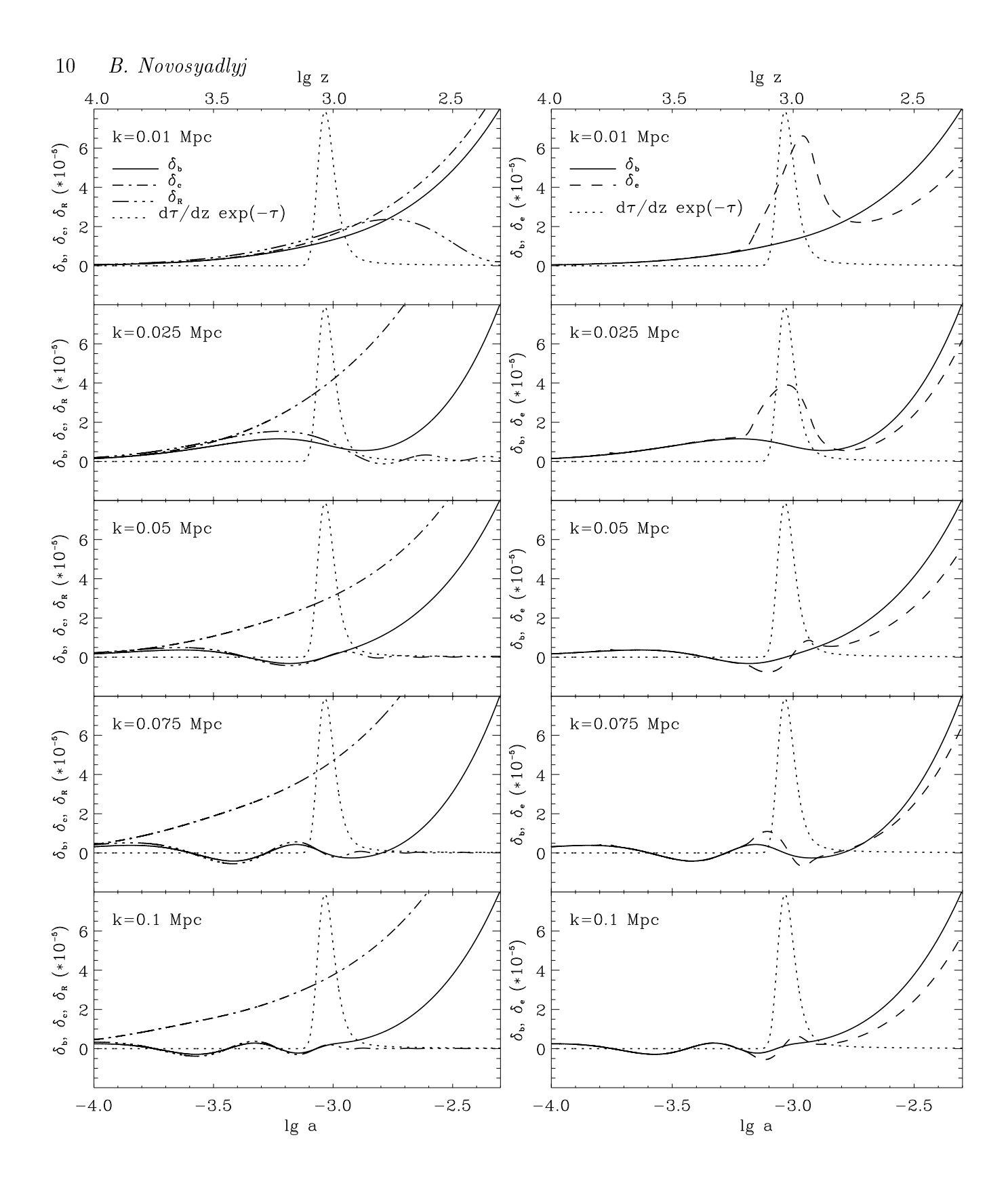


Figure 4. Left-hand column: evolution of relative density perturbations δ_b , δ_R and δ_c for the baryon (solid line), photon (dash-three dotted line) and CDM (dash-dotted line) components with adiabatic initial conditions and free normalization. Right-hand column: electron number density perturbations against baryon mass density ones. The amplitudes of all perturbations are in dimensionless units 10^{-5} . The visibility function $d\tau/dze^{-\tau}$ (multiplied by 0.018 for convenience, dotted line) denotes the position of last scattering surface.

4 Δ_E AND CORRUGATION OF LAST SCATTERING SURFACE

The results presented in Fig.2 prove that ion number density fluctuations caused by kinetics of ionization-recombination processes in the field of cosmological adiabatic perturbations do not lead to appreciable additional local temperature fluctuations. This was expected because of dominating role of the thermal (relic) electromagnetic radiation in the energy balance of photon-baryon plasma. However, to calculate of CMB temperature fluctuations and polarization at high accuracy in order to achieve better agreement between theory and observations it is necessary to take into account the contributions of such electron number density fluctuations into optical depth τ caused by Thomson scattering .

The visibility function $d\tau/dze^{-\tau}$, where $\tau(z) = \int_0^z c\sigma_T n_e(z)H^{-1}(z)(z+1)^{-1}dz$, represents the probability that a photon was scattered for the last time within dz of z. So, the main part of CMB photons come to observer from the vicinity of maximum of visibility function. The fluctuations of number density of electrons result into faint "corrugation" of last scattering surface of thermal relic radiation: the maximum of visibility function will be at somewhat lower redshifts for overdensity perturbations and at somewhat higher redshifts for underdensities than for unperturbed region. We can estimate this effect in the following way.

The redshift of peak can be determined from the condition of local extremum giving the equation:

$$\frac{1}{x_e} \frac{dx_e}{dz} - \frac{1}{H(z)} \frac{dH(z)}{dz} + \frac{2}{z+1} - \frac{c\sigma_{\rm T} n_{\rm H} x_e(z)}{H(z)(z+1)} = 0, \tag{20}$$

where $n_e(z)$ is unperturbed number density of electrons shown in Fig.1, $H(z) = H_0 \left[\Omega_{\rm R} (z+1)^4 + \Omega_m (z+1)^3 + \Omega_k (z+1)^2 + \Omega_{\Lambda} \right]^{1/2}$ is Hubble constant. Its solution for z gives a position of peak of visibility function in unperturbed medium. For Λ CDM model with the same parameters as for Fig.4 using the numerical solution we obtain $z_{dec} \simeq 1088$. In the range of perturbation, where $\hat{n}_{\rm H} = n_{\rm H}(1+\delta_b)$ and $\hat{x}_e = x_e(1+\Delta_e)$, it is expected to be $\hat{z}_{dec} = z_{dec} + \delta z_{dec}$. The displacement of peak δz_{dec} can be estimated by variation of equation (20) and expanding of functions $x_e(\hat{z}_{dec})$ and $n_{\rm H}(\hat{z}_{dec})$ into Taylor series about z_{dec} (in linear approximation):

$$\frac{\delta z}{z+1} = \left[\frac{c\sigma_{\rm T} n_{\rm H} x_e(z)}{H(z)(z+1)} (\delta_b + \Delta_{\rm e}) - \frac{d\Delta_{\rm e}}{dz} \right] \times \left[\frac{c\sigma_{\rm T} n_{\rm H} x_e(z)}{H(z)(z+1)} \left(\frac{1}{H(z)} \frac{dH(z)}{dz} (z+1) - \frac{1}{x_e} \frac{dx_e}{dz} (z+1) - 2 \right) - (z+1) \frac{d}{dz} \left(\frac{1}{H(z)} \frac{dH(z)}{dz} - \frac{1}{x_e} \frac{dx_e}{dz} \right) - \frac{2}{z+1} \right]^{-1}.$$
(21)

Therefore, such displacement depends on the amplitude of $\Delta_{\rm e} + \delta_b = \delta_e$ and the gradient of $\Delta_{\rm e}$. For arbitrary normalisation of amplitude of cosmological perturbations it is conveniently to present the result in units of relative density perturbations of baryon-photon plasma components and for large-scale perturbations $(k < k_{dec}^s)$ we have: $\delta z_{dec}/(z_{dec}+1) \approx -0.25\delta_{\rm R} = -0.33\delta_b$. If we suppose $\Delta_{\rm e} = 0$ (ion number density perturbations follow the baryon mass density ones) then $\delta z_{dec}/(z_{dec}+1) \approx -0.051\delta_{\rm R} = -0.068\delta_b$. So, the amplification of perturbation amplitudes of electron number density by recombination processes makes the last scattering surface more "corrugated" in optical depth. Such "corrugation" results into observable CMB temperature fluctuations.

We can make the estimation of this effect. Let us suppose that major part of CMB photons come from thin last scattering surface placed at z_{dec} from unperturbed medium and $\hat{z}_{dec} = z_{dec} + \delta z_{dec}$ from perturbed one. Because temperature of the thermal radiation at z_{dec} and at \hat{z}_{dec} is the same then its observable variation follows from the well-known relation $T_0 = T_{dec}/(z_{dec}+1)$: $(\delta T_0/T_0)_{cor} = -\delta z_{dec}/(z_{dec}+1) \approx 0.25\delta_{\rm R} = 0.33\delta_b$ that equals to intrinsic adiabatic CMB temperature fluctuation, $(\delta T_0/T_0)_{ad} = \delta_{\rm R}/4 = \delta_b/3$, exactly. It is other way for calculation of adiabatic term of CMB primary anisotropy, which, however, requires the accurate precalculation of Δ_e or δ_e different from δ_b at last scattering surface. When we suppose that $\delta_e = \delta_b \ (\Delta_e = 0)$ then $(\delta T_0/T_0)_{cor} \approx 0.2 \ (\delta T_0/T_0)_{ad}$ that is incorrect.

For small-scale perturbations $k > k_{dec}^s$, the value of $\delta z_{dec}/(z_{dec}+1)$ will be smaller and its sign will alternate depending on oscillation phases of δ_R and δ_b at z_{dec} . The assumption of thin LSS is too rough in this case to make correct estimation. The line-of-sight integration must be undertaken here because of fuzziness effect leading to exponential reduction of any primary CMB anisotropy. Unfortunately, straightforward substitution of recfast.f subroutine by drecfast.f one in available codes (CMBfast, CMBEASY etc.) for calculation of temperature and polarization C_l 's does not give correct estimation of possible changes to CMB power spectra caused by effect demonstrated here. It looks that collision term connected with Thomson scattering in electron density perturbed region and Boltzmann equation for photons must be generalized to take this effect into account properly. It will be the matter of the separate paper.

CONCLUSIONS

In the field of adiabatic density perturbations the rates of hydrogen and helium ionization-recombination processes slightly differ from those in the non-perturbed medium. On the one hand the rate of recombination increases due to somewhat larger number density of plasma particles in the overdense region, on the other hand the photoionization is increased too due to positive temperature initial perturbation since number density of photons capable to ionize atoms is slightly higher, rising the level of ionization. The second effect prevails at the beginning of recombination epoch and competition of effects results into the positive additional overdensity of ions and electrons. For initial perturbations with opposite sign (underdense region) all results are symmetric. The effect is prominent for large-scale initial perturbations ($k \leq k_{dec}^s$) which never oscillate acoustically.

Thus, the maximal amplitude of perturbations of proton and electron relative number density during the recombination epoch is by factor of $\simeq 5$ higher than amplitude of δ_b , baryon density perturbations. For helium it is $\simeq 18$ times higher, but practically does not influence the amplitude of perturbations of electron relative number density because of low level of ionization at z < 1200. For initial perturbations of scales inside acoustic horizon at decoupling epoch $(k \ge k_{dec}^s)$ the deviations of number density perturbations from baryon total density ones vanish owing to the temperature and density oscillations of photon-baryon plasma during recombination. They are small also for isothermal initial perturbations.

At lower redshifts, when ionization becomes residual and baryon mass density perturbation increases the electron number density perturbations δ_e becomes lesser than δ_b independently of scale of baryon density perturbation. The difference acquires $\sim 20\%$ at $z \sim 200$.

Revealed deviations of electron number density perturbations amplitudes from baryon total density ones at cosmological recombination epoch do not lead to appreciable additional local temperature fluctuations in matter or thermal radiation. But they result in faint optical depth "corrugation" of last scattering surface: $\delta z_{dec}/(z_{dec}+1) \approx -0.33\delta_b$ at scales larger than sound horizon. Taking them into account may improve the agreement between theoretical predictions and observable data of current WMAP and future PLANCK missions on large-scale CMB anisotropy and polarization.

ACKNOWLEDGMENTS

Weymann R., Phys.Fluids, 8, 2112

Wong W.Y., Seager S.& Scott D., 2005, astro-ph/0510634 Zabotin N. A., Nasel'skii P. D., 1982, SvA, 26, 272

I would like to thank Bohdan Hnatyk, Stepan Apunevych and Yurij Kulinich for useful discussions and comments. I am also grateful to Michal Ostrowsky for hospitality and possibility to work one month in Astronomical observatory of Jagellonian University, where the stimulating academic atmosphere allowed this work to progress. This work is performed in the framework of state project No 0104U002125 (Ministry of Education and Science of Ukraine).

References

Bardeen J.M., 1980, Phys. Rev.D., 22, 1882 Bennett C.L. et al., 2003, ApJS, 148, 1 Chluba J. & Sunyaev R.A., 2006, A&A, 446, 39 Durrer R., 2001, J.Phys.Studies, 5, 177 Drake G.W.F., Victor G.A., & Dalgarno A., 1969, Phys.Rev., 180, 25 Dubrovich V.K. & Grachev S.I., 2005, AstL, 31, 359 Goldman S.P., 1989, Phys.Rev. A, 40, 1185 Hinshaw G. et al., 2003, ApJS, 148, 135 Hu W. & Sugiyama N., 1995, ApJ, 444, 489 Hummer D. G., & Storey P. J., 1998, MNRAS, 297, 1073 Jones B. J. T., & Wyse R. F. G., 1985, A&A, 149, 144 Kholupenko E.E., Ivanchik A.V. & Varshalovich D.A., 2005, Grav. & Cosmology (Rus), 11, 161 Kodama H. & Sasaki M., 1984, Prog. Theor. Phys. Suppl., 78, 1 Krolik J. H., 1990, ApJ, 353, 21 Liubarskii Iu. E. & Sunyaev R. A., 1983, A&A, 123, 171 Ma C.-P. & Bertschinger E.,-1995, ApJ, 455, 7 Matsuda T., Sato H., & Takeda H., 1971, Prog. Theor. Phys., 46, 416 Peebles P. J. E., 1968, ApJ, 153, 1 Péquignot D., Petitjean P., & Boisson C., 1991, A&A, 251, 680 Rubicki G. B. & Dell'Antonio I. P., 1993, ApJ, 427, 603 Schramm D.N. & Turner M.S., 1998, Rev.Mod.Phys., 70, 303 Seager S., Sasselov D.D. & Scott D., 1999, ApJ, 523, L1 Seager S., Sasselov D.D. & Scott D., 2000, ApJS, 128, 407 Seljak U., Zaldarriaga M., 1996, ApJ, 469, 437 Silk J., 1968, ApJ, 151, 459 Spergel D.N. et al., 2003, ApJS, 148, 175 Spergel D.N. et al., 2006, astro-ph/0603449 Tegmark M., Strauss M.A., Blanton M.R et al., 2004, Phys.Rev. D, 69, 103501 Verde L. et al., 2003, ApJS, 195, 195 Verner D. A. & Ferland G.J., 1996, ApJS, 103, 467

Zaldarriaga M., Seljak U., 1999, ApJS, 29, 431 Zel'dovich Ya. B., Kurt V. G., & Sunyaev R. A., 1968, Zh. Eksp. Teoret. Fiz., 55, 278

Table A1. Atomic constants and coefficients of approximation formulae

Constant	Value	Source	Formula
χнι	$2.17871122 \cdot 10^{-18} \text{ J}$	Seager et al. (1999)	(3),(15)
χ_{HeI}	$3.9393393 \cdot 10^{-18} \text{ J}$	Seager et al. (1999)	(2), (14)
XHeII	$8.71869443 \cdot 10^{-18} \text{ J}$	Seager et al. (1999)	(1),(13)
$h\nu_{ m H2s}$	$1.63403509 \cdot 10^{-18} \text{ J}$	Seager et al. (1999)	(7),(18)
$h\nu_{ps}$	$3.30301387 \cdot 10^{-18} \text{ J}$	Seager et al. (1999)	(5),(17)
$h\nu_{ m HeI2^1s}$	$9.64908312 \cdot 10^{-20} \text{ J}$	Seager et al. (1999)	(5),(17)
$h\nu_{2s-1s}$ (HI)	$5.4467613 \cdot 10^{-19} \text{ J}$	Péquignot et al. (1991)	(9)
$n\nu_{2s-1s}$ (HeII)	$6.36325429 \cdot 10^{-19} \text{ J}$	Hummer & Storey (1998)	(9)
$\lambda_{ m H2p}$	121.567 nm	Seager et al. (1999); Verner & Ferland (1996)	(7),(18)
$\lambda_{ m HeI2^1p}$	58.4334 nm	Seager et al. (1999); Verner & Ferland (1996)	(5),(17)
F	1.14	Seager et al. (1999)	(8)
a	4.309	Péquignot et al. (1991)	(8)
b	-0.6166	Péquignot et al. (1991)	(8)
С	0.6703	Péquignot et al. (1991)	(8)
d	0.5300	Péquignot et al. (1991)	(8)
q	$1.80301774 \cdot 10^{-17}$	Hummer & Storey (1998)	(6)
p	0.711	Hummer & Storey (1998)	(6)
T_1	$1.30016958 \cdot 10^5 \text{ K}$	Hummer & Storey (1998)	(6)
T_2	3K	Hummer & Storey (1998)	(6)
$\Lambda_{ m H}$	$8.22458 c^{-1}$	Goldman (1989)	(7),(18)
$\Lambda_{ m He}$	$51.3 \ c^{-1}$	Drake et al. (1969)	(5),(17)

APPENDIX A: THE VALUES OF ATOMIC CONSTANTS AND COEFFICIENTS OF APPROXIMATION FORMULAE USED IN NUMERICAL CALCULATIONS